Complex-Coherence Measurements for Lensless Object Positioning

H. Esat Kondakci[1,*], Ahmed El-Halawany[1], Andre Beckus[2], Nafiseh Mohammadian[1], George K. Atia[2], and Ayman F. Abouraddy[1]

[1]*CREOL, The College of Optics & Photonics, University of Central Florida, Orlando, FL 32816, USA*
[2]*Dept. of Electrical and Computer Engineering, University of Central Florida, Orlando, FL 32816, USA*
[*]*esat@creol.ucf.edu*

Abstract: We experimentally demonstrate complex-coherence function of incoherent light intercepted by a one-dimensional object in various configurations. By examining only the coherence function, we determine the axial and transverse position and size of the object.

© 2017 Optical Society of America

OCIS codes: (030.1640) Coherence; (120.3180) Interferometry; (030.6600) Statistical optics

Coherence is a universal wave phenomenon describing the correlation properties of wave packets at the same or different points in space and time and can be measured through alternative settings such as Michelson interferometer, Mach-Zehnder interferometer, and Young's double slit experiment in the case of electromagnetic waves [1]. Coherence properties of a light field depends on many factors, e.g., the propagation distance, nature of the source, medium the field propagates through, and the scattering objects along the path of the propagation. Each of these effects and perturbations to the propagating field leaves its fingerprints on the complex coherence function [2].

Here, we demonstrate measurement of complex-coherence function of incoherent LED light passing through one-dimensional (1D) objects. To measure the coherence function, we implement Young's double slit experiment [3, 4] for various slit separations with a computer-controlled digital-micro-mirror device [5, 6] (Fig. 1). We are particularly interested in the regime where the shadow of the incoming light disappears (i.e., the observation plane is at the far field) and intensity is approximately uniform. Considering a single-scattering object (in the form of an obstruction to the field or a reflective object), we find that measuring the spatial coherence enables identification of the transverse and axial location of the scatterer and its size. This technique paves the way to object positioning that are hidden around a corner with no direct sight since the complex-coherence characteristics of an incoherent field may be partially preserved even if it reflects from scattering media such as a wall. Another advantage of this technique is that the sampling in the

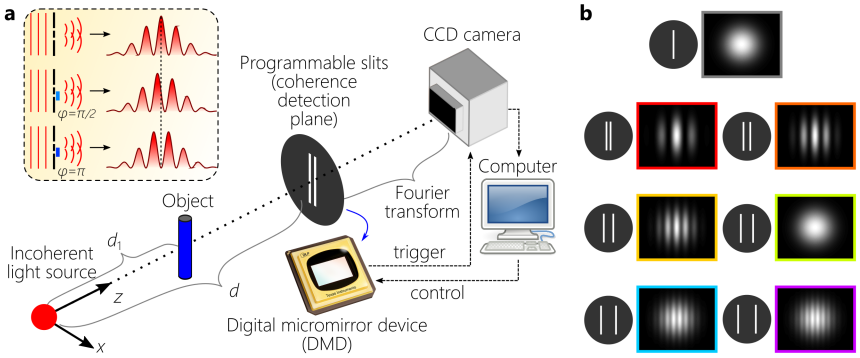

Fig. 1. The concept of the complex-coherence measurement of scattered incoherent light. (a) The schematic of the experimental setup. Incoherent light (LED) with a center wavelength of 630 nm scatters through a one-dimensional (1D) object and impinges on the computer-controlled double slits. From the double slits to the CCD camera, spatial Fourier transform is implemented. The inset depicts the effect of relative phase on the interference pattern for spatially coherent monochromatic light. For a relative phase of $\phi = \pi$, the intensity at the center becomes minimum. (b) Spatially and spectrally partially-coherent light results in interference patterns with reduced visibility depending on the separation of double slits, the spectral bandwidth and the interaction of the propagating field with the object along the propagation path.

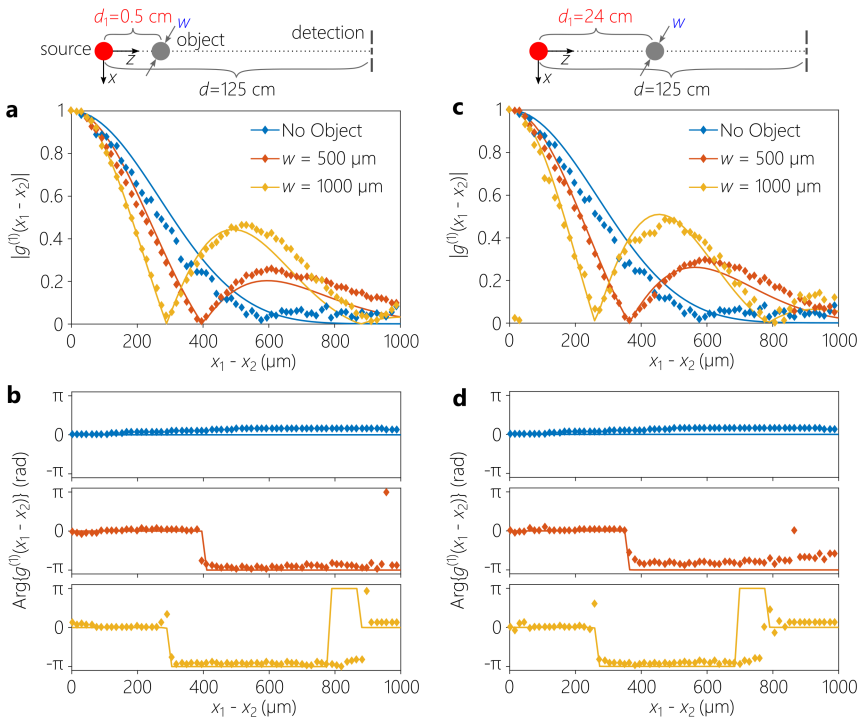

Fig. 2. The effect of object's size and axial position on the complex-coherence function $g^{(1)}(x_1 - x_2)$. (a) The magnitude and (b) phase of the coherence function for two object widths (in comparison to the no-object case) at a fixed source to object distance of 0.5 cm. (c,d) Same as in (a,b) except for object to source distance of 24 cm. (a-d) The theory is shown as a solid line, whereas the experimental results are plotted with diamonds.

detection plane is only required for a limited spatial extent in the order of the transverse coherence width enabling space limited applications.

The measurement of the complex-coherence function is conceptually depicted in Fig. 1. The inset shows the effect of relative phase in a double slit experiment and this effect is the basis of our analysis to extract the phase information at a given slit separation. The double slits are realized via digital micromirror device (DMD, Texas Instruments DLP6500). To obtain interference patters, Fourier transform is realized along the horizontal direction x by means of free-space propagation. In the actual experiment, the slits are realized in reflection mode and the Fourier transform is realized with a pair of lenses for optical relay (and spatial filtering) and a cylindrical lens (for focusing along the vertical direction), which are omitted in the schematic in Fig.1 for simplicity. In all cases we report here, we plot the magnitude and phase of the normalized second-order field correlation as a function of slit separation given by

$$g^{(1)}(x_1 - x_2) = \langle E^*(x_1)E(x_2)\rangle / \langle \sqrt{I(x_1)I(x_2)}\rangle, \tag{1}$$

where $E(x_1)$ is the electromagnetic field at x_1, $I(x_1)$ is the intensity at x_1, and $\langle\ \rangle$ is for the time and spectral averaging inherent in the CCD measurement of the scattered LED source.

The first scenario we consider is that of an intercepting object located at $x = 0$ for two different distances along the propagation direction z and two object sizes $w = 500, 1000\ \mu$m and we compare these cases to the case where the object is absent (Fig. 2). In the absence of an object, the coherence function smoothly goes to zero [Fig. 2(a)] with no significant phase change [Fig. 2(b)]. However, intercepting the field with an object introduces a side lobe in the magnitude of $g^{(1)}$ and π-phase shift at the starting point of the first side lobe. The position of the phase-shift point depends on the object's width and position. Increasing the object's size results in a shift towards lower coherence lengths for starting point of the side lobe. This effect is also enhanced when the object is placed further away than the source [Fig. 2(c),(d)]. We also observe another phase jump (back to zero phase after wrapping) at the starting point of the secondary side lobe in the coherence function.

Figure 3 depicts the complex-coherence function for different axial [Fig. 3(a),(b)] and transverse [Fig. 3(c),(d)] positions of an object with a fixed width ($w = 500\ \mu$m). As the distance from the source to the object increases, the

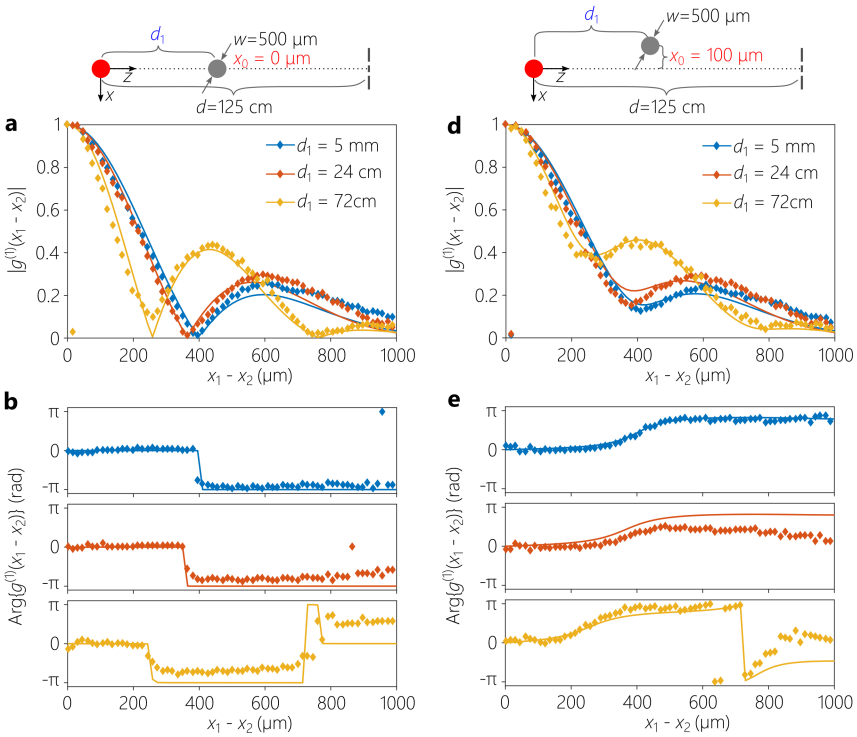

Fig. 3. The effect of object's axial and transverse position on the complex-coherence function $g^{(1)}(x_1 - x_2)$. (a)The magnitude and (b) phase of the coherence function for a fixed object width of 500 μm at three axial distances. (c,d) Same as in (a,b) except for different transverse positions. (a-d) The theory is shown as a solid line, whereas the experimental results are plotted with diamonds.

starting point of the side lobe takes place at lower coherence lengths. This behavior resembles the effect of increasing size of the object shown in Fig. 2. However, there is a significant tell-tale sign in this case to differentiate the two cases from each other. In this case, the difference between the starting points of the first and secondary lobes gets smaller.

The effect of offset position in the transverse direction is shown in Fig. 3(c),(d). In this case, there are significant changes both in the magnitude of the coherence function $g^{(1)}$ and its phase. In this case, even though there are apparent dips in the coherence function at the expected locations (based on the size and axial position of the object), the dips do not reach to zero [Fig. 3(c)]. As a result of this smooth transition, the phase does not exhibit sudden phase jumps, instead there is a smooth transition as shown in Fig. 3(d).

In conclusion, we showed the effect of various objects on the coherence function of an incoherent light source. We demonstrated that although the information in the intensity profile is lost, the coherence function retains useful information. In addition, the coherence function remains localized, and therefore the detection plane can be restricted to a small region. In this work, we particularly considered the tracking of three object parameters: transverse position, longitudinal position, and width.

References

1. B. E. A. Saleh and M. C. Teich, *Principles of Photonics*, (Wiley, 2007).
2. L. Mandel and E. Wolf, *Optical Coherence and Quantum Optics*, (Cambridge University, 1995).
3. A. F. Abouraddy, K. H. Kagalwala, and B. E. A. Saleh, "Two-point optical coherency matrix tomography," Opt. Lett. **39**, 2411 (2014).
4. K. H. Kagalwala, H. E. Kondakci, A. F. Abouraddy, and B. E. A. Saleh, "Optical coherency matrix tomography," Sci. Rep. **5**, 15333 (2015).
5. H. Partanen and J. Turunen, and J. Tervo, "Coherence measurement with digital micromirror device," Opt. Lett. **39**, 1034 (2014).
6. G. Vdovin, H. Gong, O. Soloviev, P. Pozzi, and M. Verhaegen, "Lensless coherent imaging by sampling of the optical field with digital micromirror device," J. Opt. **17**, 122001 (2015).